

Rheological Behavior of a Dispersion of Small Lipid Bilayer Vesicles

K. H. de Haas, C. Blom, D. van den Ende,* M. H. G. Duits, B. Haveman, and J. Mellema

J. M. Burgers Centre, Rheology Group, Department of Applied Physics, University of Twente, P.O. Box 217, 7500 AE Enschede, The Netherlands

Received May 29, 1997. In Final Form: October 3, 1997

Rheological behavior of a dispersion of small nearly-unilamellar phospholipid bilayer vesicles has been investigated. We conducted steady-state shear experiments and linear viscoelastic experiments. In the dilute and semidilute regime the rheological behavior is similar to that of a hard-sphere dispersion as reported in the literature for viscoelastic measurements, but now also observed in steady shear experiments. The effect of the main acyl-chain phase transition, taking place at 23 °C, can be described with an increase of the effective volume fraction. As a result, with temperature variation one can obtain effective volume fractions larger than the maximum packing fraction for hard spheres. Near and above the maximum packing fraction a dynamic yield stress τ_y and a frequency independent storage modulus G' develop. In this concentration regime the rheological behavior is determined by the interplay between vesicle deformation and the intervesicle interaction, and so far, there is no indication which phenomenon is dominant. A comparison with recently reported measurements suggests that G' is proportional to a^{-3} , where a is the vesicle radius. Furthermore, we show that $\tau_y \approx \gamma_c G'$ which is in agreement with theory. Here τ_y is the dynamic yield stress and γ_c the critical strain which indicates the transition to nonlinear behavior in a viscoelastic experiment. There is a striking resemblance between our high concentration results and those reported in literature for vesicles in the so-called onion phase. To the best of our knowledge this is the first rheological study for concentrated nearly-unilamellar vesicle dispersions with volume fraction and temperature as variables.

I. Introduction

The aim is to investigate the rheological behavior of a dispersion of lipid bilayer vesicles as a function of volume fraction and temperature. A vesicle is a liquid droplet with a surface membrane that consists of one (unilamellar) or more (multilamellar) lipid bilayers. In this investigation where the lipid dimyristoylphosphatidylcholine (DMPC) has been used, the majority of vesicles is close to unilamellar and has an average radius of about 250 nm.

The rheological behavior of a dispersion of vesicles depends on the interaction between vesicles and the vesicle deformability. The interactive forces between vesicles can be distinguished in a hydrodynamic force and several static forces. Unavoidably there is the attractive van der Waals force and a repulsive force as a result of excluded volume. For small lipid bilayer vesicles, a small amount of charge-carrying molecules usually has to be introduced to prevent aggregation; hence an electrostatic repulsive force is also present. Furthermore, there can be an entropic repulsion as a result of the presence of thermal undulations at the bilayer interface. The deformability is determined by the interplay between the mechanical properties of the lipid bilayer, the magnitude of the interfacial area, and the number of bilayers in the vesicle interface.

The mechanical properties of lipid bilayers depend strongly on temperature. Several phases are distinguished corresponding to different states of the acyl chains.¹ Lipid bilayers are in the so-called gel state when temperature is below the main acyl-chain phase transition temperature, which is $T_c = 23$ °C for DMPC. In this state the lipid tails are aligned rigidly constituting an ordered solid-like state. Above the transition temperature the

bilayer is in the liquid-crystalline or fluid state. The lipid bilayer has melted, so the lipids are disordered and move freely through the bilayer. The bilayer area has increased by about 20% and the bilayer thickness has decreased by about 20%. Two pre-transitions can occur prior to the melting transition.

The first rheological experiments on vesicle dispersions were conducted by Smeulders et al.^{1a,2} They performed linear viscoelastic measurements on dispersions of egg yolk vesicles with the bilayer in the fluid state.^{2a,2b} Three relaxation processes were observed, where the one at lowest frequency was of entropic nature like that observed in hard-sphere dispersions and the other two were related to vesicle deformation. Smeulders et al. also measured the shear viscosity of a vesicle dispersion consisting of a mixture of saturated lipids with an acyl-chain phase transition temperature of 51 °C.^{1a,2c} Near this phase transition temperature a sharp viscosity rise was observed, probably due to a lipid area increase.

In this paper we report a study of the steady-state shear viscosity and the linear viscoelastic behavior of dilute, semidilute, and densely packed vesicle dispersions as a function of shear rate and temperature. These experiments are supported by dynamic light scattering experiments and freeze-fracture electron micrographs. Our findings are compared with experimental results found in literature for unilamellar and multilamellar vesicles. Furthermore, we discuss the microscopic structure of a vesicle dispersion in relation to its rheological behavior.

Recently, studies were published on the rheological behavior of concentrated multilamellar vesicle dispersions,³ where the volume fraction of a vesicle sample in this so-called onion phase is difficult to determine. For our vesicle dispersions we are able to determine an

* Author to whom correspondence should be addressed.

© Abstract published in *Advance ACS Abstracts*, November 15, 1997.

(1) (a) Smeulders J. B. A. F. The mechanical properties of lipid bilayers. Ph.D. Thesis, The Netherlands, 1992. (b) Evans, E.; Needham, D. *J. Phys. Chem.* **1987**, *91*, 4219. (c) Cevc, G.; Marsh D. *Phospholipid Bilayers*; John Wiley & Sons: New York, 1987.

(2) (a) Smeulders, J. B. A. F.; Mellema, J.; Blom, C. *Phys. Rev. A* **1992**, *46*, 7708. (b) Smeulders, J. B. A. F.; Blom, C.; Mellema, J. *Phys. Rev. A* **1990**, *42*, 3483. (c) Smeulders, J. B. A. F.; Mellema, J.; Blom, C. Proceedings of the XIth International Congress on Rheology, Brussels, 1992; p 738.

effective hard-sphere volume fraction and we can vary this volume fraction. Thus this study may contribute to the understanding of the rheological behavior of this onion phase.

The paper is organized as follows: In section II we give a theoretical treatment of the static vesicle interactions and a brief review on the viscosity of hard-sphere dispersions. This is our starting point, as deviations from hard-sphere behavior indicate the influence of vesicle interaction and vesicle deformability. In section III we discuss our vesicle system. Freeze-fracture electron micrographs give insight in the vesicle size distribution, the number of bilayers in the vesicle interfaces, and the vesicle shape. In section IV we first present the shear viscosity as a function of shear rate and temperature and linear viscoelastic experiments for samples with very high volume fractions are described. Eventually, in section V we end with some conclusions.

II. Theory

A. Vesicle Interaction. Reviews on the possible interactions in a dispersion of lipid bilayer vesicles have been presented on several occasions.^{1c,4} We distinguish the following types of vesicle interaction: van der Waals attraction (w), electrostatic repulsion (e), and a "long-range" entropic repulsion as a result of thermal undulations (u). We assume them to be additive and write the interaction energy as a function of distance d between the vesicle surfaces:

$$\Phi(d) = \Phi_w(d) + \Phi_e(d) + \Phi_u(d) \quad (1)$$

At very short bilayer separations a repulsive hydration force is also present which should be taken into account when the bilayers are uncharged. We follow the approach of Lipowski and Leibler.⁵ For the sake of simplicity the interaction energy (per unit of area) of two parallel flat bilayers is considered. The aim of this approach is to get a rough estimate of the strengths of the different interactive forces, which gives a qualitative picture of the macroscopic properties of the vesicle dispersions.

The van der Waals interaction energy between two parallel flat bilayers is

$$\Phi_w(d) = -\frac{A_H}{12\pi} \left[\frac{1}{d^2} - \frac{2}{(d+h)^2} + \frac{1}{(d+2h)^2} \right] \quad (2)$$

with A_H the Hamaker constant and $h \approx 5$ nm the bilayer thickness. For lipid bilayers in water the Hamaker constant is about $(5 \pm 2) \times 10^{-21}$ J.^{1c,6}

Since the van der Waals attraction may cause flocculation of the vesicles, a vesicle dispersion is commonly stabilized by adding a small amount of charged molecules which are incorporated in the lipid bilayer. Generally, the vesicles are dispersed in a z-z electrolyte solution, while the liquid inside the vesicle has the same composition. The electrostatic interaction energy between two parallel flat charged membranes can be given by⁷

$$\Phi_e(d) = 64kTn_b\kappa^{-1} \tanh^2\left(\frac{1}{4}\Psi_s\right) \exp(-\kappa d) \quad (3)$$

where k is Boltzmann's constant, T is temperature, n_b is the electrolyte concentration, Ψ_s is the dimensionless electrostatic potential at the vesicle surface, and κ is the reciprocal Debye length. This is the result of linear superposition of two isolated plates with constant charge and is valid for $\kappa d \gg 1$. The reciprocal Debye length is given by

$$\kappa^2 = \frac{2z^2 e^2 n_b}{\epsilon \epsilon_0 kT} \quad (4)$$

with e the electron charge, ϵ the relative dielectric constant of water, and ϵ_0 the dielectric constant in vacuum. In our vesicle dispersion we estimate $n_b = 0.13$ M while $z = 1$, so $\kappa \approx 0.8$ nm.

The dynamics of an undulating vesicle surface has been described by several authors.⁸ We use the description presented by Helfrich and Servuss.^{8a} They give the interaction energy between two separate flat undulating membranes

$$\Phi_u(d) \propto \frac{(kT)^2}{k_c d^2} \quad (5)$$

with k_c the bending rigidity of the lipid bilayer. This expression is based on the interaction energy between an undulating membrane and a rigid surface. For that specific case the proportionality constant can be derived. This proportionality constant was estimated to be near unity,^{8a} but a Monte Carlo simulation predicts a value that is of order 0.1.⁹ In order to have a noticeable contribution of the undulation interaction, the distance d has to be so small that the amplitudes of the undulations of each bilayer are affected by the presence of the other bilayer. The mean square amplitudes of the undulations of a single isolated bilayer depend on the total amount of excess area (or the effective surface tension) and the bending rigidity.

Compared to the other two interactions, the decay of the electrostatic interaction with d is rapid. Figure 1 shows the estimated interaction energies as a function of the bending rigidity. Variations of the Hamaker constant or the dimensionless electrostatic potential at the vesicle surface give no qualitative change of their dependence on the bilayer separation. A value $k_c \approx 10^{-19}$ J corresponds to the DMPC literature values for the fluid state.¹⁰ Larger values for k_c are also shown, to illustrate the possible behavior of lipid bilayers in the gel state or for multilayered bilayers. We see that for the lowest value of k_c , the entropic repulsion is dominant so the bilayers repel each other. For higher values of k_c , the van der Waals attraction and the electrostatic repulsion become dominant and an attractive potential well results.

The range of d in which eq 5 is valid cannot be sharply defined. It should be related to the mean square amplitudes of the undulations. In the fluid state there is an amount of excess area of about 20%. Estimations of the mean square undulation amplitudes^{8a,b} show that for

(3) (a) Versluis, P.; van de Pas, J. C.; Mellema J. *Langmuir*, in press. (b) Hoffmann, H.; Thunig, C.; Schmiedel, P.; Munkert, U. *Langmuir* **1994**, *10*, 3972. (c) Hoffmann, H.; Thunig, C.; Schmiedel, P.; Munkert, U. *Nuovo Cimento Soc. Ital. Fis., D* **1994**, *16*, 1373. (d) Panizze, P.; Roux, D.; Vuillaume, V.; Lu, C. Y. D.; Cates, M. E. *Langmuir* **1996**, *12*, 248.

(4) Jones, M. N. *Adv. Colloid Interface Sci.* **1995**, *54*, 93.

(5) Lipowski, R.; Leibler, S. *Phys. Rev. Lett.* **1986**, *56*, 2541.

(6) Marra, J.; Israelachvili, J. N. *Biochemistry* **1985**, *24*, 4608.

(7) (a) Russel, W. B.; Saville, D. A.; Schowalter, W. R. *Colloidal Dispersions*; Cambridge University Press: Cambridge, 1989. (b) Bell, G. M.; Levine, S.; McCartney, L. N. *J. Colloid Interface Sci.* **1970**, *33*, 335.

(8) (a) Helfrich, W.; Servuss, R. M. *Nuovo Cimento Soc. Ital. Fis., D* **1984**, *3*, 137. (b) Milner, S. T.; Safran, S. A. *Phys. Rev. A* **1987**, *36*, 4371. (c) Seifert, U. *Z. Phys. B* **1995**, *97*, 299.

(9) Seifert, U. *Phys. Rev. Lett.* **1995**, *74*, 5060.

(10) (a) Engelhardt, H.; Duwe, H. P.; Sackmann, E. *J. Phys. Lett.* **1985**, *46*, 395. (b) Evans, E.; Rawics, W. *Phys. Rev. Lett.* **1990**, *64*, 2094 (c) Duwe, H. P.; Sackmann, E. *Physica A* **1990**, *163*, 410. (d) Beblík, G.; Servuss, R. M.; Helfrich, W. *J. Phys.* **1985**, *46*, 1773.

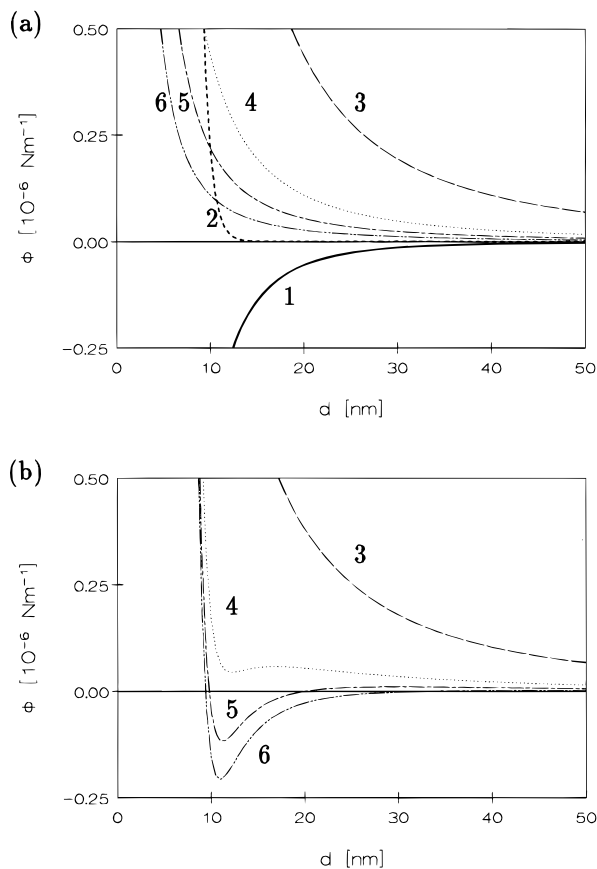


Figure 1. Different types of interaction energies (per unit of area) as a function of bilayer separation are shown in (a). The following interactions are distinguished: van der Waals attraction with $A_H = 5 \times 10^{-21}$ J (1), electrostatic repulsion with $\Phi_s = 1$ (2), and entropic repulsion with $k_c = 10^{-19}$ J (3), $k_c = 4 \times 10^{-19}$ J (4), $k_c = 8 \times 10^{-19}$ J (5), and $k_c = 16 \times 10^{-19}$ J (6). (b) The sum of the van der Waals energy, the electrostatic energy, and the entropic energy with variation of k_c . The symbols are the same as in (a).

vesicles with radii of about 250 nm this equation is probably valid for bilayer separations up to several tens of nanometers. For lipid bilayers in the gel state the amount of excess area is smaller and the bending rigidity is possibly somewhat larger, so the mean square undulation amplitudes are smaller. Thus, for lipid bilayers in the gel state, eq 5 is valid for smaller bilayer separations than for bilayers in the fluid state, and possibly the entropic repulsion is negligible which results in an effective attraction between the bilayers.

B. Microscopic Structure of a Vesicle Dispersion.

Previously it was mentioned that at high volume fractions the vesicle interactions and the vesicle deformability may both contribute to the macroscopic behavior of a vesicle dispersion and that they are influenced by each other. In this section this is illuminated by considering the interaction energy and the elasticity of the bilayers.

The total energy of the system is the sum of the interaction energy and the energy stored in the lipid bilayers. In the previous section a relation for the interaction energy has been given. The interfacial energy of a vesicle is given by the following integral over the vesicle surface¹¹

$$\Phi = \int \left(\sigma + \frac{1}{2} k_c (C - C_0)^2 \right) dA \quad (6)$$

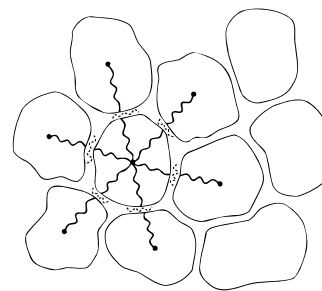


Figure 2. Schematic representation of the microstructure of a highly concentrated vesicle dispersion. The influences on the elasticity of the entire dispersion by the vesicle interaction (---) and the vesicle deformability (—) are symbolized by different sets of springs.

with σ the surface tension, C the local curvature of the membrane, and C_0 the natural curvature of the lipid bilayer.

In the absence of vesicle interactions the average vesicle shape follows from energy minimization of eq 6. This is the case in a dilute dispersion of vesicles. For higher volume fractions, the vesicle interactions come into play. Both the deformation energy and the interaction energy and, therefore, the total energy increase. How much energy is stored in deformation and how much in interaction depends on the strength of both and is not known a priori. Figure 2 shows a schematic representation of the microstructure of a highly-concentrated vesicle dispersion. Here the interaction and the elasticity are symbolized by two different sets of springs.

To understand the rheological behavior of a concentrated dispersion of vesicles, one needs a model for the microstructure under flow. In this model the average vesicle shape as a function of the flow rate should play an essential role. For several reasons it is difficult to calculate the shape of the vesicles. First, the spatial distribution of the vesicles has to be known in order to account for the influence of each neighbor vesicle. Secondly, the “contact area” between two vesicles has to be defined, and the interbilayer distance is not constant in this area, so the parallel-membrane approximation has to be adjusted. Furthermore, the thermal undulations are affected by vesicle deformation, which has its impact on the applicability of eqs 1 and 6.

Speaking in terms of the set of springs in Figure 2, the rheological behavior depends on the spring moduli that pertain to vesicle deformation and on those pertaining to vesicle interaction. These moduli depend on the volume fraction, shear rate, and the degree of deformation. We did not attempt to come to a complete microrheological model but considered two limiting cases that are simple enough for a quantitative approach: a dispersion of non-deformable interacting vesicles and a dispersion of deformable vesicles where the only interaction is that of excluded volume. In the next section these limiting cases are elucidated.

C. Linear Viscoelastic Behavior of a Vesicle Dispersion.

In a linear viscoelastic experiment the complex shear viscosity $\eta^*(\omega) = \eta'(\omega) - i\eta''(\omega)$ and the complex shear modulus $G^*(\omega) = i\omega\eta^*(\omega) = G'(\omega) + iG''(\omega)$ are obtained as a function of angular frequency ω in a certain range of frequencies. The viscosity is usually made dimensionless by division through the solvent viscosity η_s giving the relative dynamic viscosity $\eta_r^* = \eta^*/\eta_s$. In the remainder of this paper the relative viscosity is used, unless otherwise stated.

For volume fractions in the range of $0.25 < \phi < 0.5$ the linear viscoelastic behavior of a vesicle dispersion has been investigated by Smeulders et al.^{2a,b} For lipid bilayers in

(11) Helfrich, W. *Z. Naturforsch., C* **1973**, *28*, 693.

the fluid state three mechanical relaxation processes are observed experimentally. The relaxation process at lowest frequency corresponds to diffusive behavior of the vesicles and is also observed in hard-sphere dispersions, see van der Werff et al.¹² The other two relaxation processes have been related to vesicle deformation. The Oldroyd model¹³ appeared to be a useful tool for understanding their mechanisms. The relaxation process at highest frequencies is related to the surface dilatation modulus and the other one to the dynamic surface shear modulus.^{2a,14}

In the previous section we announced the relation of the microstructure of the vesicle dispersions to the macroscopic rheological properties for two limiting cases. First, we gave a description of undeformable interacting particles. Then we gave a description of a dispersion of deformable vesicles that only have excluded volume interaction. For both cases an estimated value for the storage modulus G' is obtained.

When the volume fraction of a dispersion becomes that high that the average repulsive interaction energy between undeformable particles is on the order of $3/2kT$ or more, a phase transition can take place. For effectively monodisperse spheres a face-centered cubic (fcc) or a body-centered cubic (bcc) phase can be expected.¹⁵ Otherwise the structure resembles that of an amorphous solid. In either case a storage modulus G' independent of ω is expected. In literature the following relation between the pair-interaction energy and this storage modulus has been used by several authors^{15,16}

$$G' = \frac{\phi_m N}{5\pi(2a + d)} \left[\frac{\partial^2 \Phi}{\partial d^2} + \frac{\partial \Phi}{\partial d} \left(\frac{4}{2a + d} \right) \right] \quad (7)$$

with ϕ_m the maximum packing fraction, which depends on the type of ordering of the particles, N the number of nearest-neighbor particles, a the particle radius, and Φ the pair-interaction energy.

We will use eq 7 assuming that the vesicle interaction is dominated by repulsion due to thermal undulations. From eqs 5 and 7 we derive the storage modulus in the limit $\phi \rightarrow 1$. The interaction energy in eq 5 is given per unit of area, so it is multiplied with a^2 to obtain an approximate relation for the pair-interaction energy. The assumption that in reality vesicles are deformable allows $\phi_m \approx 1$ and $N \approx 10$. In a monodisperse dispersion the average distance between the vesicle surfaces is

$$\bar{d} = 2a \left[\left(\frac{\phi_m}{\phi} \right)^{1/3} - 1 \right] \quad (8)$$

In practice the distance between the vesicle surfaces is determined by a force balance, so this equation is only a crude estimate. Substitution of eqs 5 and 8 into eq 7 gives

$$G' = \text{Order} \left(\frac{(kT)^2}{10k_c a^3} [\phi^{-1/3} - 1]^{-4} \right) \quad (9)$$

This estimation probably predicts an upper-limit value because eq 8 is an overestimation due to polydispersity

(12) van der Werff, J. C.; de Kruif, C. G.; Blom, C.; Mellema, J. *Phys. Rev. A* **1989**, *39*, 795.

(13) (a) Oldroyd, J. G. *Proc. R. Soc. London, Ser. A* **1953**, *218*, 122. (b) Oldroyd, J. G. *Proc. R. Soc. London, Ser. A* **1955**, *232*, 567.

(14) de Haas, K. H.; Ruiter G. J.; Mellema, J. *Phys. Rev. E* **1995**, *52*, 1891.

(15) van der Vorst, B.; van den Ende, D.; Mellema, J. *J. Rheol.* **1995**, *39*, 1183.

(16) (a) Buscall, R.; Goodwin, J. W.; Hawkins, M. W.; Ottewill, R. H. *J. Chem. Soc., Faraday Trans. 1* **1982**, *78*, 2889. (b) Wagner, N. J. *J. Colloid Interface Sci.* **1993**, *161*, 169.

and the estimation of the contact area a^2 is too large near and below the maximum packing fraction.

Our second limiting-case model for the storage modulus is based solely on the deformation of vesicles in a shear flow. The storage modulus is then a measure of the average energy that is stored in the deformation of vesicles (per unit of volume). The energy that is stored in an arbitrary deformation of a vesicle has been described by Milner and Safran.^{8b} The physically relevant parameters are the bending rigidity k_c and the surface tension σ . The relation between the storage modulus and the energy that is stored in a deformed emulsion droplet with an interfacial tension has been elaborated by Mellema et al.¹⁷ Following their procedure for the case of vesicles at low concentrations, the relation between G' and ϕ becomes

$$G' = \text{Order} \left(\max \left[\left(\frac{k_c}{a^3} \right), \left(\frac{\sigma}{a} \right) \right] \right) \quad (10)$$

For low-volume fractions G' depends only weakly on ϕ . At high-volume fractions it may depend strongly on ϕ , because of the influence of the vesicle shapes. Application of eq 10 in this concentration regime results in an estimation of a lower bound for the storage modulus.

D. Shear Viscosity of a Vesicle Dispersion. The viscosity of a dispersion of undeformed noninteracting vesicles resembles that of hard spheres. A repulsive interaction force can be accounted for in effective vesicle radii that are slightly larger than the real vesicle radii when the concentration is not very high. Deviations from hard sphere behavior are possible when the vesicles aggregate as a result of an attractive interaction,^{7a} when the average vesicle distance is so small that the static vesicle interaction comes into play, or when the vesicle deforms as a consequence of applied shear stress.

Aggregation results in a viscosity increase, and generally shear-thinning behavior is observed.^{7a} The influence of interaction forces in combination with deformation of the vesicles by the shear forces is a rather complex subject, and no attempt has been made to come to a predictive model. In a recent paper¹⁸ a deformation model is presented; it is based on flattening of the thermal undulations as a result of the decrease of excess area. This is caused by a transition from a spherical to an ellipsoidal vesicle shape. When the model is applied to our vesicle dispersion, it predicts no significant vesicle deformation in the shear-rate range of $0.01 < \dot{\gamma} < 100 \text{ s}^{-1}$. For a shear stress $\eta_e \dot{\gamma} \approx 10^4 \text{ Pa}$ or higher, deformation might be significant; here, η_e is the dispersion viscosity. According to this model vesicle deformation might play a role only at very high volume fractions. Thus, we expect that for a broad range of volume fractions and shear rates our vesicle system behaves as an effective hard-sphere dispersion.

The shear viscosity of monodisperse hard-sphere dispersions has been investigated by several authors. For a dilute dispersion of hard spheres the viscosity is given by Einstein's classical equation

$$\eta_r = \frac{\eta}{\eta_s} = 1 + \frac{5}{2} \phi \quad (11)$$

with η_r the relative viscosity and η the viscosity.

Usually, the volume-fraction dependence of η_r at moderate to high volume fractions is represented by a

(17) Mellema, J.; Blom, C.; Beekwilder, J. *Rheol. Acta* **1987**, *26*, 418.

(18) de Haas, K. H.; Blom, C.; van den Ende, D.; Duits, M. H. G.; Mellema, J.; Submitted.

semiempirical function. Several authors^{19,20} found that over the entire range from a dilute dispersion to a volume fraction near the maximum packing fraction ϕ_m , the viscosity can be represented adequately by Quemada's expression²¹

$$\eta_r = \left(1 - \frac{\phi}{\phi_m}\right)^{-2} \quad (12)$$

Following van der Werff and De Kruif, we chose $\phi_m = 0.63$ in the low shear limit and 0.71 in the high shear limit.

The viscosity of a hard-sphere dispersion is a function of shear rate, with a Newtonian plateau at low shear rates at η_0 , a plateau at high shear rates at η_∞ , and an intermediate shear-thinning region. The difference between both plateaus is the viscosity contribution of the Brownian motion of the spheres. van der Werff and de Kruif¹⁹ found the following empirical expression

$$\eta_r(\dot{\gamma}) = \eta_\infty + \frac{c}{\dot{\gamma}} \left[1 - \exp\left(-\frac{\eta_0 - \eta_\infty}{c} \dot{\gamma}\right)\right] \quad (13)$$

where c is a constant related to the critical shear rate $\dot{\gamma}_c$: $\eta_r(\dot{\gamma}_c) = 1/2(\eta_0 + \eta_\infty)$. A more convenient expression for $\dot{\gamma}_c$ is the characteristic Peclet number

$$Pe_c = \frac{a^2 \dot{\gamma}_c}{D_0} \quad (14)$$

where $D_0 = kT/6\pi\eta_s a$ is the translational diffusion coefficient of a sphere and a the sphere radius. This characteristic Peclet number is a function of volume fraction.¹⁹

III. Materials and Methods

A. Preparation and Handling of DMPC Vesicle Dispersions. For moderate volume fractions the characteristic Peclet number in eq 14 is of order unity.¹⁹ In order to observe the Brownian transition in a steady-state shear experiment, the critical shear rate has to be $\dot{\gamma}_c \approx 1$. This can be achieved with a vesicle radius of several hundreds of nanometers. There are different methods listed in literature for the preparation of small vesicles. In this study the vesicles are prepared with the detergent removal method,²² which is known to generally yield narrow size distributions, at a controllable size. We have developed a recipe to obtain DMPC vesicles of an average radius of about 250 nm.

The DMPC lipids (Lipid Products Ltd.) are used without further purification. An amount of 750 mg of DMPC lipids is dissolved in 100 mL of a 2:1 mixture of chloroform and methanol. To stabilize the vesicle dispersion, a charge carrier in a molar ratio of 0.2 with respect to the lipids is added to the solution. We used the Tris salt of cholesteryl hemisuccinate (Sigma Chemical Co.). An amount of 950 mg of the detergent sodium cholate (Sigma), which can be dissolved in water and has affinity with the lipids, is added in pure form to this solution. This detergent has only one apolar tail. The solvent is evaporated under reduced pressure, and a thin dry film results on the inside of a round-bottomed flask. Next, the film is dissolved in 66 mL of an aqueous phosphate buffer of pH 7.4 and

osmolarity of 0.26. A clear mixed-micelles solution is formed. This solution is dialyzed for 24 h against the phosphate buffer. The detergent is slowly removed from the mixed-micelles solution and now the vesicles are formed. During the dialysis process the solution is kept at 31 °C. This is well above the phase transition temperature $T_c = 23$ °C of the bilayer. Each synthesis results in 66 mL of vesicle dispersion with a volume fraction of about 0.15.

In an Amicon Ultra Filtration device the dispersion is concentrated to higher volume fractions. During the filtration process, temperature is kept at 10 °C, well below the phase transition temperature. Volume fractions in the range of 0.5–0.6 are obtained with the concentration process. Volume fractions in the range 0.25–0.5 can be made by dilution of these samples with the phosphate buffer.

In order to retard biological degradation, our vesicles are stored at 4 °C, where the vesicle dispersion appears white and turbid. Samples stored at 37 °C appear yellow and clear. A criterion for a stable vesicle dispersion is that no sedimentation is observed. Occasionally we observed sedimentation for a sample that was stored below T_c : after a few days a clear phase is observed on top of the white phase. Samples that sedimented were not used in our experiments. An interesting observation is that when a sedimented dispersion is heated to above the transition temperature, the vesicles redisperse to a clear yellow dispersion.

This phenomenon indicates that for lipid bilayers in the gel state there is probably an attraction between vesicles, which disappears for fluid lipid bilayers. This might indicate that at temperatures above T_c the repulsive undulation energy is larger and below T_c it is smaller or of the same order of magnitude as the van der Waals energy. As mentioned in section IIA, below T_c undulation amplitudes are probably very small because the amount of excess area is much smaller and the bending rigidity is possibly larger.

The shear viscosity of freshly prepared vesicle samples at volume fractions of about 0.15 is almost independent of shear rate at temperatures both below and above T_c . However, for freshly prepared vesicle dispersions that show sedimentation after some time, shear thinning is observed, and for shear rates of about 0.01 s^{-1} the viscosity may be 1 or more orders of magnitude larger than that of stable samples. Due to this correlation between sedimentation at rest and shear thinning behavior, measurement of the shear-flow curve is a quick method to investigate the stability of a vesicle dispersion.

When the samples are concentrated by ultrafiltration below T_c and the resulting volume fraction is close to maximum packing, shear thinning is observed below T_c . When this sample is diluted to its original volume fraction, this shear-thinning behavior remains, while the original sample at the same volume fraction has an almost constant viscosity. We think that the forces involved in the concentration process may cause a breakup and redistribution of the lipid bilayers. Such a redistribution may decrease the stability of the dispersions if vesicles become more multilamellar. This suppresses thermal undulations. Therefore, we distinguish between two different vesicle dispersions, one that has a history of moderate volume fractions (type I) and another which was concentrated to a volume fraction near maximum packing (type II).

B. Freeze-Fracture Electron Micrographs. In Figure 3 we show freeze-fracture electron micrographs of two volume fractions of the same vesicle dispersion (type II). The effective volume fractions are $\phi_r = 0.43$ and ϕ_l

(19) van der Werff, J. C.; de Kruif, J. C. *J. Rheol.* **1989**, *33*, 421.

(20) Phan, S. E.; Russel, W. B.; Cheng, Z.; Zhu, J.; Chaikin, P. M.; Dunsmuir, J. H.; Ottewill, J. R. *Phys. Rev. E* **1996**, *54*, 6633.

(21) Quemada, R. *Lecture Notes in Physics: Stability of Thermodynamic Systems*, Cases-Vasquez J.; Lebon, J., eds.; Springer: Berlin, 1982; p 210.

(22) Zumbühl, O.; Weder, H. G. *Biochim. Biophys. Acta* **1981**, *640*, 252.

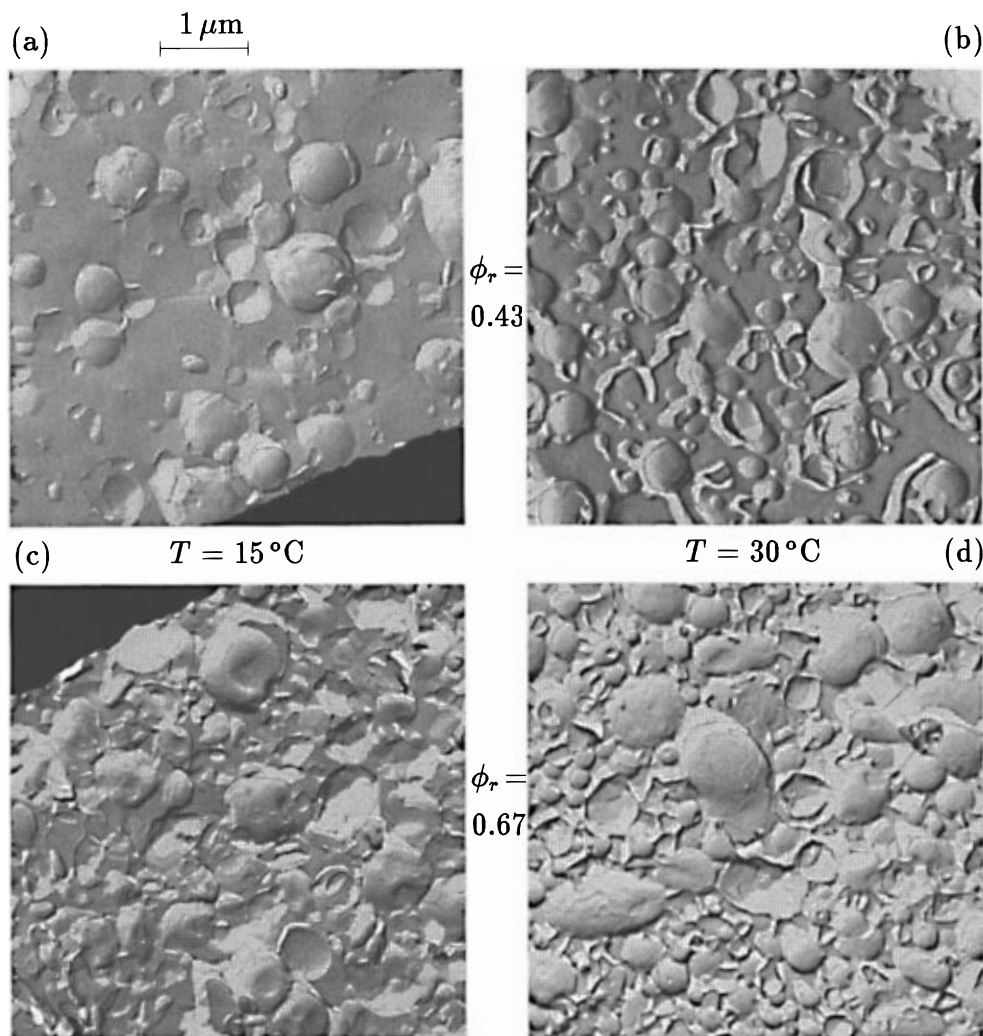


Figure 3. Freeze-fracture electron micrographs of vesicle dispersions of type II. The phase transition from the L_{β} phase to the L_{α} phase is shown for two volume fractions. (a) $\phi_r = 0.43$, $T = 15$ °C. (b) $\phi_r = 0.43$, $T = 30$ °C. (c) $\phi_r = 0.67$, $T = 15$ °C. (d) $\phi_r = 0.67$, $T = 30$ °C.

$= 0.67$. The index r indicates that these are reference values, which are the average volume fractions below T_c that have been determined with the method described in section IVA. The samples are frozen from $T = 15$ °C and $T = 30$ °C. The freeze-fracture method and the microscope technique are described by Versluis et al.^{3a}

The electron micrographs show that there is a topological difference between the gel state and the liquid-crystalline phase. Most striking are the sharper vesicle surfaces below T_c . This is consistent with the presence of significant thermal undulations above T_c . Below T_c and at lowest ϕ_r the vesicle shape is approximately spherical. However, for the highest volume fraction some vesicles are deformed due to the presence of neighboring vesicles. At $T = 30$ °C a higher fraction of nonspherical shapes is observed. This might result from larger excess area of the lipid bilayer when temperature is larger than T_c .

Many vesicles seem to have an interface that consists of a few bilayers instead of one. Also a number of vesicles have encapsulated another vesicle. The vesicle dispersions are rather polydisperse. Vesicle radii in the range of 20–600 nm are observed at 15 °C and radii in the range of 10–700 nm are observed at 30 °C. The broadness of the size distribution is slightly overestimated, because the cross sections of the vesicles are not necessarily through the vesicle centers. It is expected that the average vesicle radius is larger when temperature is larger than T_c . This

is correct for the largest vesicles but apparently not for the smallest ones. The most frequently appearing vesicle radius is about 300 nm at 15 °C and 260 nm at 30 °C. The detergent removal method usually gives radii in the range of 40–100 nm.^{1a,2b,22} Our vesicle radii are substantially larger so there is no experimental basis for expecting to obtain unilamellar and monodisperse vesicles.

In Figure 3a, the vesicles are grouped together, which is another indication for a net attractive force between vesicles at temperatures below T_c . In Figure 3b the vesicles appear to be connected too, but the distribution is more random. The connections appear to be nonvesicular. On the basis of measurements of the shear viscosity at low and moderate concentrations, it was argued in the previous section that the net attractive force below T_c has changed to a repulsive force above T_c . So above T_c the connecting bilayer structures are probably transient or very loose.

C. Dynamic Light Scattering. It is common to determine the hydrodynamic radius of spherical particles by dynamic light scattering. With this method we have determined the average vesicle radius to be about 250 nm. This is in agreement with the electron micrographs. Smeulders et al.^{1a,2c} measured the vesicle radius as a function of temperature. They showed that the main acyl-chain phase transition can be visualized by an increase of the hydrodynamic vesicle radius. Our vesicles do not show this behavior as a function of temperature. This

might be due to the higher polydispersity of our vesicle dispersion, which makes interpretation more difficult. In the previous section it appeared that large vesicles become larger but small vesicles become smaller when temperature is increased. This complex behavior is not accounted for in the data analysis. Smeulders et al. observed a hysteresis in the apparent vesicle radius when the temperature sweep is followed by a temperature decrease below T_c . We have not observed this hysteresis with our DMPC vesicles.

D. Rheological Measurements. The steady-state shear viscosity of the vesicles has been measured with a Contraves LS-40 device with a Couette geometry. It is known that evaporation may result in a thin elastic film at the dispersion-to-air interface. In a conventional geometry this influences the apparent viscosity. Therefore a home-made vapor-lock and a guard ring were used. The geometry is filled with 1 mL of vesicle dispersion. The shear-rate range is 2×10^{-4} to 100 s^{-1} . We measured the shear viscosity as a function of shear rate, with temperature and concentration as independent parameters. For each sample the first measurement was done at 10°C , and in successive measurements, temperature was increased in steps of 5°C up to 40°C . The measuring time, including an average delay time of 20 min on average, of each step is about 1 h. For a few samples temperature was subsequently decreased, again in steps of 5°C . Reproducibility was further checked through repetition of the entire experiment with a few freshly introduced samples, and for each measurement the shear rate sweep was carried out in both directions.

As no hysteresis was observed for type I or type II vesicles, there is no indication for influence of shear stress on the size of the vesicles during the experiments, in contrast to the observations of Roux et al.²³ This can be due to the fact that type I vesicles are unilamellar and vesicles of type II are supposed to be nearly unilamellar, while during filling the highest shear rates are obtained so at that stage the size of the vesicles will be determined.

The linear viscoelastic experiments have been carried out with a home-made instrument²⁴ with a double-gap geometry. We have selected this device because of its sensitivity and the frequency range of 0.001–50 Hz, and because it is equipped with a vapor lock. The geometry is filled with 9 mL of vesicle dispersion. Once more, temperature was varied between 10 and 40°C . Reproducibility was tested for some samples by repeating the experiment and also by applying an upward as well as a downward temperature sweep.

IV. Experimental Results

A. Steady-State Shear Viscosity. In Figure 4 we show the relative viscosity of a vesicle dispersion of type I for two volume fractions as a function of temperature. There is a large and sharp viscosity increase when temperature is increased through the acyl-chain phase transition temperature of 23°C . Not surprisingly, this effect is larger for larger volume fractions. For each sample the relative viscosities at 10 and 15°C nearly coincide, as well as the viscosities between 25 and 40°C . For relatively low viscosities, a Newtonian plateau is visible at small shear rates, while at high shear rates the onset to a high-shear-rate plateau can be observed. For higher viscosities the shear-thinning region broadens and the Newtonian plateau is no longer observed at small shear

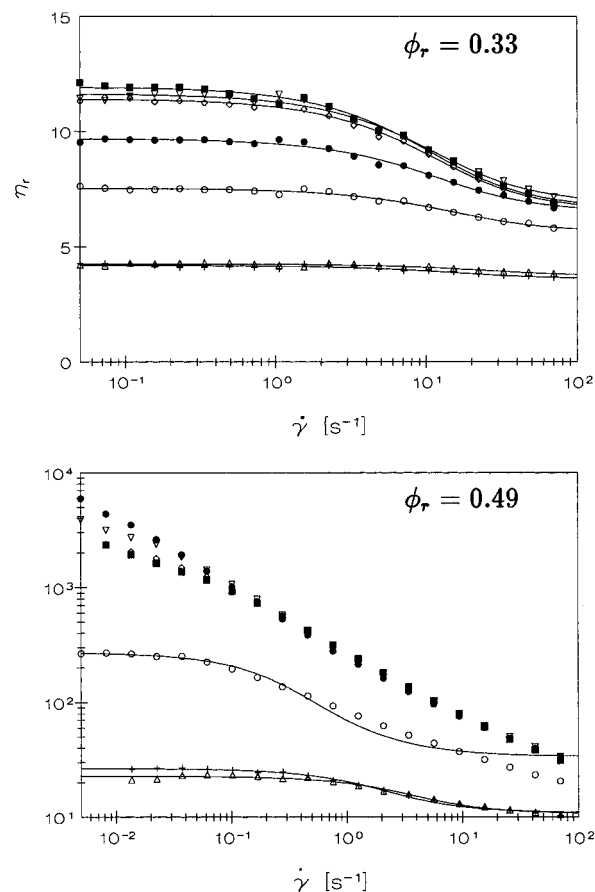


Figure 4. Shear viscosity as a function of shear rate for two volume fractions of vesicle dispersions of type I. Temperatures are 10°C (+), 15°C (Δ), 20°C (\circ), 25°C (\bullet), 30°C (∇), 35°C (\diamond), and 40°C (\blacksquare). The fits with van der Werff's empirical expression are shown. Note that the first figure has a linear viscosity scale, whereas the second one has a logarithmic scale.

rates. The transition between the plateaus is the vanishing contribution of Brownian motion, due to a changing particle position distribution. For high volume fractions this transition is dominated by a different microstructural change, which might be related to the details of the interaction at short surface-to-surface distance and the vesicle deformability.

Hereafter, we show that for low volume fractions the viscosity of a vesicle dispersion resembles that of a hard-sphere dispersion. Equation 12 has been substituted into eq 13 with $\phi_m = 0.63$ for the low-shear plateau and $\phi_m = 0.71$ for the high-shear plateau. Thus, η_0 and η_∞ are eliminated and only the fitting parameters ϕ and c remain. We recall that ϕ can a priori only be estimated from the synthesis procedure. The fit results are shown in Figure 5. It is clear that the curves containing viscosity plateaus can be fitted well for relative viscosities up to at least 30.

We have also fitted our measurements with eq 13 where the coupling between both viscosity plateaus is not incorporated. This method results in a more accurate determination of η_0 and η_∞ . In Figure 5 these values are shown for all fits on vesicle dispersions of type I, where the effective volume fraction has been retrieved from the first fitting procedure. Deviations of η_0 and η_∞ from Quemada's theoretical expression indicate a discrepancy with hard-sphere behavior. For effective volume fractions up to 0.5, both η_0 and η_∞ are close to these theoretical lines. This figure contains data from all temperatures. We have not observed a significant difference between data below and above T_c . Figure 5 contains a few dilution

(23) (a) Roux, D.; Nallet, F.; Diat, O. *Europhys. Lett.* **1993**, *24*, 53 (b) Diat, O.; Roux, D. *J. Phys. II* **1993**, *3*, 9. (c) Diat, O.; Roux, D.; Nallet, F. *J. Phys. II* **1993**, *3*, 1427.

(24) Zeegers, J.; van den Ende, D.; Blom, C.; Altena, E. G.; Beukema, G. J.; Mellema, J. *Rheol. Acta* **1995**, *34*, 606.

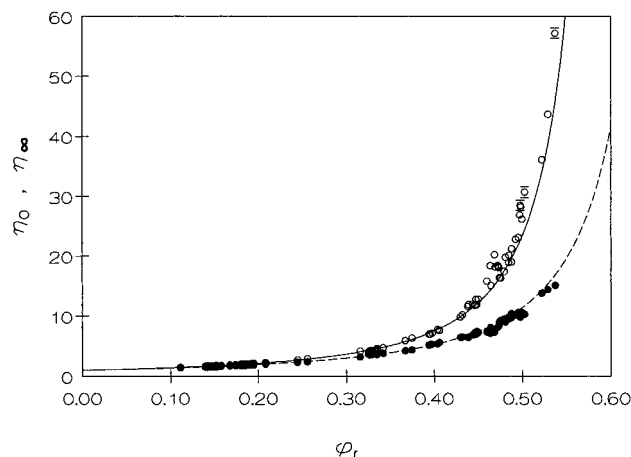


Figure 5. Estimation of the effective volume fractions for all type I dispersions with low viscosities. The theoretical lines according to Quemada's expression are drawn with $\phi_m = 0.63$ for the low-shear rate plateaus (—) and $\phi_m = 0.71$ for the high-shear rate plateaus (- -). η_0 denoted by open symbols and η_∞ denoted by solid symbols.

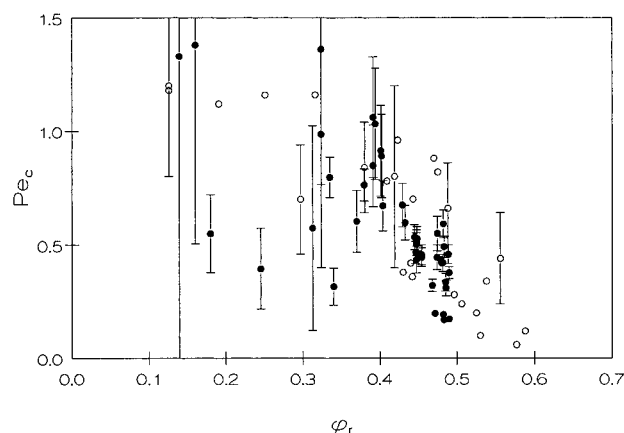


Figure 6. Characteristic Peclet number as a function of volume fraction for type I vesicle dispersions, solid symbols, and hard sphere dispersions (van der Werff and de Kruijff¹⁹), open symbols.

series, and we have revealed that the ratios of the volume fractions that follow from the fits agree well with the ratios of dilution.

We use eq 14 to calculate the characteristic Peclet number Pe_c for each measurement. Figure 6 shows Pe_c for our vesicle dispersions and the hard-sphere dispersions of van der Werff and de Kruijff.¹⁹ For all measurements we have used a vesicle radius of 250 nm in eq 14, and it appears that our results are in close agreement with those of hard-sphere dispersions.

These findings imply a convenient procedure to determine an estimated volume fraction based on the measured shear viscosity. Throughout this paper, the volume fractions have been determined with this method. Unless otherwise stated, the given volume fraction ϕ_r of a vesicle dispersion is the average value below the phase transition temperature, and it is considered as the reference value. When the low-shear plateau cannot be observed, volume fractions have been assigned, using the dilution factor to the concentration of a diluted sample where the hard sphere fit was still possible. We should keep in mind that our volume fraction is that of an effective hard-sphere dispersion. The real volume fraction is the total volume of the vesicle interiors and that of the lipid bilayers divided by the total dispersion volume. The real volume fraction is essentially constant, assuming that diffusion of solvent through the lipid bilayers is negligible on the time scale of the experiment. The effective hard sphere

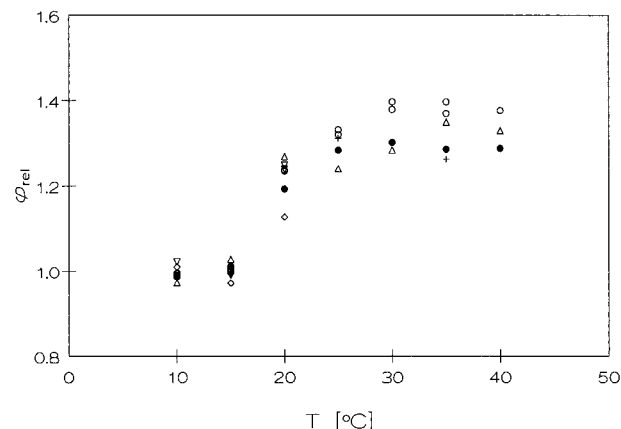


Figure 7. Increase of the relative hard sphere volume fraction with temperature for type I vesicle dispersions. Average volume fractions below 20 °C are $\phi_r = 0.15$ (+), $\phi_r = 0.25$ (Δ), $\phi_r = 0.33$ (\circ), $\phi_r = 0.38$ (\bullet), $\phi_r = 0.40$ (∇), and $\phi_r = 0.49$ (\diamond). For the two highest volume fractions there are no data points above 20 °C.

volume fraction is based on the hydrodynamic radius, which depends on the vesicle shape and the interaction forces. Furthermore, the polydispersity is not accounted for. For this reason, the choices $\phi_m = 0.63$ for the low-shear plateau and $\phi_m = 0.71$ for the high-shear plateau may be underestimated, and therefore the resulting effective volume fractions too.

The lipid phase transition can be illuminated when the effective volume fraction is plotted versus temperature. This is shown in Figure 7. The volume fractions are relative to the reference volume fraction. The average error is $\Delta\phi_{rel} \approx 0.05$. It is clear that the ϕ_{rel} increases by about 30% when temperature is increased beyond T_c . The real area increase of the lipid bilayers is expected to be 20% as well as the effective area increase. The phase transition appears to begin just below 20 °C, while the expected value of the main transition temperature is 23 °C.

In summary, for relative viscosities at least up to 30 our vesicle system behaves as an effective hard-sphere system. The plateaus at low and high shear rates, as well as the characteristic Peclet numbers, are in close agreement with literature values.

B. Steady-State Shear Viscosity for High Volume Fractions. In the previous section it was suggested that for high volume fractions the vesicle interaction and deformability influence the shear viscosity. In this section, we discuss several observations that can be related to this.

In Figure 4, a slight decrease in η_0 is observed with increasing temperature at temperatures below T_c for $\phi_r = 0.49$. In section IIA it was mentioned that below T_c the van der Waals attraction and the entropic repulsion induced by thermal undulations are probably of the same order of magnitude. The entropic repulsion becomes stronger with increasing temperature as a result of the main acyl-chain phase transition and the pretransitions, because the amount of excess area increases and the bending rigidity becomes possibly smaller. We think that at 10 °C there is, as a result of both interactions, a weakly attractive force between vesicles which causes the viscosity rise. The repulsive entropic force increases with temperature and it gradually overcomes the van der Waals attraction, so the viscosity drops.

Figure 8 shows the shear viscosity of a type II vesicle dispersion. Its reference volume fraction is 0.58 ± 0.05 . Below T_c there is a strong shear-thinning behavior. At 20 °C the viscosity profile is close to that of a hard-sphere dispersion and above T_c there is once more strong shear-

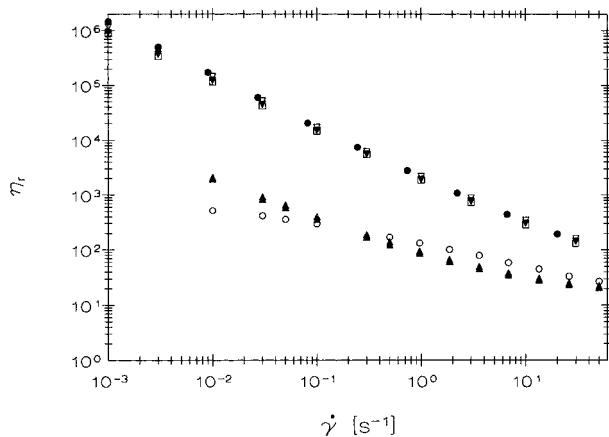


Figure 8. Relative shear viscosity as a function of temperature for $\phi_r = 0.58 \pm 0.05$ of a type II vesicle dispersion. Temperatures are 10 °C (Δ), 15 °C (\blacktriangle), 20 °C (\circ), 25 °C (\bullet), 30 °C (∇), 35 °C (\blacktriangledown), and 40 °C (\square). The data of 10 and 15 °C nearly coincide.

thinning behavior, where the shear stress is almost constant across the entire shear rate range. The strong shear thinning below T_c reflects that the effective attractive force is much stronger for a type II dispersion than for a type I dispersion; see section IIIA. This observation explains our choice for distinguishing between these two vesicle dispersion types. As in the case for a type I dispersion the strength of the resulting attraction is slightly decreasing with increasing temperature. A consequence of this shear-thinning effect, which is also seen for diluted samples, is that the volume fraction cannot be determined from a viscosity measurement below T_c . However, above T_c this method is still applicable, because above T_c the diluted type II samples again display the effective hard sphere behavior. For this reason we use Figure 7 to estimate the reference volume fractions for type II dispersions below T_c , thereby unavoidably increasing its uncertainty.

C. Linear Viscoelasticity of a Vesicle Dispersion.

We have carried out linear viscoelastic experiments for type II vesicle dispersions. A steady-state shear experiment has been performed simultaneously with exactly the same samples to determine the sample volume fractions and allow a comparison between both experiments.

Figure 9 shows the real part of the dynamic viscosity η'_r and the storage modulus G' for $\phi_r = 0.58 \pm 0.05$ as a function of frequency and temperature. This volume fraction is close to the maximum packing fraction for hard spheres. The shear viscosity of this sample has been discussed in the previous section. As for the shear viscosity, a sharp transition is observed for η'_r and G' when temperature increases beyond T_c . At constant frequency both G' and η'_r , taken as a function of temperature, display a minimum near 20 °C. This indicates that at this temperature the weak effective attraction between the vesicles, which is dominant at lower temperatures, is balanced by a repulsive force. Above T_c the dynamic modulus G' is almost frequency independent in the entire frequency range. Under the same conditions the shear stress is nearly constant for shear rates smaller than 1 s^{-1} as can be observed from Figure 8. This latter, so-called dynamic yield stress τ_y is about 1 order smaller than the storage modulus.

The shear rate dependence of η_r and the frequency dependence of η'_r are qualitatively the same. From the experiments performed by Smeulders et al.^{2a,b} we know that two relaxation processes pertaining to vesicle deformation take place at high frequencies that are well

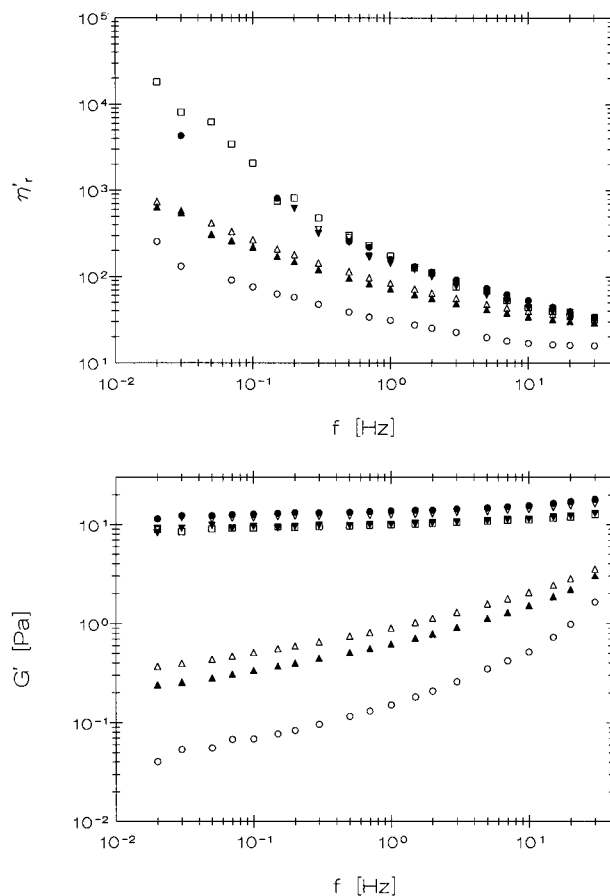


Figure 9. Real part of the dynamic viscosity η'_r and the dynamic storage modulus G' as a function of frequency for $\phi_r = 0.58 \pm 0.05$ of a type II vesicle dispersion. Temperatures are 10 °C (Δ), 15 °C (\blacktriangle), 20 °C (\circ), 25 °C (\bullet), 30 °C (∇), 35 °C (\blacktriangledown), and 40 °C (\square).

outside our measuring range. In Figure 9 the onset to another plateau for G' is visible for all temperatures at high frequencies. This probably pertains to one of these relaxation processes.

Recently, some viscoelastic experiments on densely packed multilamellar vesicles, in the so-called onion phase,³ have been reported. It is interesting that the results are qualitatively the same as for the example in Figures 8 and 9 at temperatures for $T > T_c$. For the onion phase the plateau value for G' is on the same order of magnitude and the value for G' is about 1 order smaller than G' which is also the case for our system. Furthermore, the dynamic yield stress extracted from the shear flow curve is about 1 decade smaller than the storage modulus. Our vesicles are nearly unilamellar and the interiors are filled with solvent, while the vesicles in the onion phase are completely filled with stacked bilayers.

Figure 10 shows the real part of the relative dynamic viscosity η_r^* as a function of volume fraction at 25 °C. For the lowest volume fractions the low-shear limit of the shear viscosity is added. As expected, the low-frequency limit of η_r^* is close to the low-shear limit of η_r . For low-volume fractions a relaxation transition is observed near $f = 1 \text{ Hz}$. This pertains to a Brownian relaxation process, which was investigated extensively by Smeulders et al.^{2a,b} Our findings are in close agreement with their results. Thus, for low-volume fractions our vesicle dispersions behave similar to effective hard-sphere dispersions, also with respect to their viscoelastic behavior.

From our measurements with the three highest volume fractions displayed in Figure 10 we can calculate the plateau values for G' as a function of temperature. The

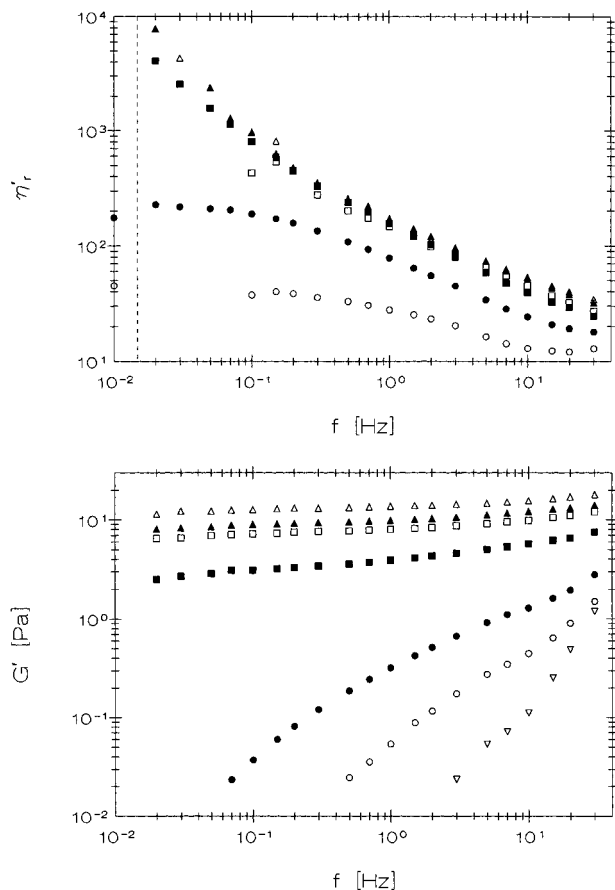


Figure 10. Relative dynamic viscosity η'_r and the storage modulus G' for a type II vesicle dispersion at $T = 25$ °C. The low shear limit of the shear viscosity is added to the left of the separation line. Volume fractions (below T_c) are $\phi_r = 0.58$ (Δ), $\phi_r = 0.55$ (\blacktriangle), $\phi_r = 0.54$ (\square), $\phi_r = 0.50$ (\blacksquare), $\phi_r = 0.45$ (\bullet), $\phi_r = 0.41$ (\circ), and $\phi_r = 0.28$ (∇).

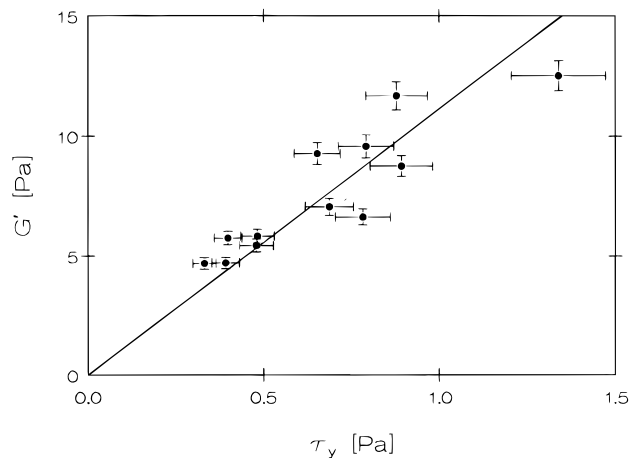


Figure 11. Relationship between the plateau values of the storage modulus G' and the dynamic yield stress τ_y for the three highest volume fractions of type II vesicle dispersions at all four temperature points above T_c .

same is valid for the plateau values of the dynamic yield stress τ_y from our steady-state shear experiments. Figure 11 shows the relation between G' and τ_y . A linear fit results in $\tau_y = (0.089 \pm 0.004)G'$. In a linear viscoelastic experiment, the applied strain needs to be so small that the dynamic moduli are independent of its magnitude. The critical strain value γ_c for which the viscoelastic behavior becomes nonlinear can be estimated from

$$\tau_y \approx \gamma_c G' \quad (15)$$

For each measurement we have verified this linearity for $f = 1$ Hz. From this we obtain $\gamma_c = 0.075 \pm 0.015$. This value is in agreement with the linear relation displayed in Figure 11. The same observation was made by Versluis et al.^{3a} for dispersions of multilamellar vesicles. They found values in the range $0.12 \leq \gamma_c \leq 0.2$.

D. Application of G' Models for Two Limiting Cases. In section IIC we mentioned two limiting cases that enable estimation of the storage modulus of a highly-concentrated vesicle dispersion. In this section we compare these models with the plateau values for G' from Figure 10, which are on the order of 10 Pa.

The first limiting case is that of undeformable interacting vesicles. The storage modulus is estimated with eq 9. The smallest volume fractions (above T_c) that give rise to a constant storage modulus are $\phi \approx 0.6$, and the highest volume fractions used in our experiment are $\phi \approx 0.8$. The assumptions $k_c = 10^{-19}$ J and $a = 250$ nm give a value $1 < G' < 30$ Pa. This means that the repulsive force which results from thermal undulations can give a significant contribution to the storage modulus.

The second limiting case is that of vesicles only interacting at contact, where the storage modulus is related to energy of deformation by eq 10. With the same assumptions for the numerical values of k_c and a as in the former limiting case, the term in eq 10 that is related to the bending rigidity predicts $G' \approx 6$ Pa. Application of the term that is related to the surface tension is more difficult, because the surface tension is unknown. It may vary between 10^{-9} and 10^{-5} N m⁻¹.²⁵ Therefore the prediction of G' varies between 10^{-3} and 10 Pa. In a forthcoming paper Gradzielski et al.²⁶ present linear viscoelastic experiments on vesicles with radii of order 15 nm. Their G' is about 3 orders of magnitude larger than ours. Assuming that the k_c values of both vesicle systems are approximately the same, the relationship $G' \propto a^{-3}$ is supported. Therefore, if the storage modulus is related to the deformation of the vesicles, the bending rigidity is probably the relevant parameter. In summary both limiting cases result in a reasonable prediction for the values of the storage modulus. Thus, at this point we cannot decide whether the vesicle interactions are responsible for these plateau values or the vesicle deformation or both.

V. Conclusions

We have investigated the rheological behavior of dispersions of nearly-unilamellar DMPC vesicles with an average radius of 250 nm. The results are compared with previous experiments with unilamellar vesicle dispersions and reported measurements on onion-like vesicles. The main advantage of our vesicle system compared to onion-like vesicles is that we have a convenient method to determine the effective volume fraction and thereby monitor the volume fraction which facilitates the interpretation. We have varied volume fraction at constant temperature and temperature at constant volume fraction.

We have distinguished between dispersions that were concentrated to moderate volume fractions (type I) and to volume fractions near the maximum packing fraction (type II). The micrographs of type II dispersions show that the vesicles are not monodisperse and that their interfaces may consist of a few bilayers. The method of preparation is generally known to give monodisperse unilamellar

(25) (a) Kummrow, M.; Helfrich, W. *Phys. Rev. A* **1991**, *44*, 8356. (b) Kwok, R.; Evans, E. *J. Biophys.* **1981**, *35*, 637.

(26) Gradzielski, M.; Bergmeier, M.; Müller, M.; Hoffmann, H. *J. Phys. Chem.*, in press.

vesicles, but during the concentration process a possible redistribution of lipid material may take place.

For volume fractions up to 0.5 the rheological behavior of the vesicle dispersions resembles that of hard-sphere dispersions. For linear viscoelastic experiments this was also observed.^{2a,b} To our knowledge, this is the first extensive treatment on the shear viscosity of vesicle dispersions. The main acyl-chain phase transition manifests itself as an effective volume fraction increase of about 30%. For high-volume fractions this gives a large viscosity increase. As a result, temperature variation is a means to obtain effective volume fractions larger than the maximum packing fraction for hard spheres.

For type II vesicle samples and for samples that were rejected because they were unstable, the shear viscosity is much larger at low volume fractions and below T_c than its expected value from hard-sphere behavior, and also strong shear-thinning behavior is observed. From these observations and our consideration of the different interaction energies, we conclude that the entropic repulsive force due to thermal undulations is larger than the van der Waals attraction for fluid lipid bilayers. However, lipid bilayers in the gel state probably have an entropic repulsion and a van der Waals attraction of approximately the same order of magnitude. The phase transition displays a change of the vesicle interaction from a weak attraction below T_c to a repulsion above T_c .

For high-volume fractions near or above the maximum packing fraction for hard spheres a dynamic yield stress appears in a steady-state shear experiment and within the measurement range the storage modulus G' becomes nearly constant in a linear viscoelastic experiment. A comparison with recent experiments reported in literature suggests that the storage modulus scales with the vesicle radius a by $G' \propto a^{-3}$. Furthermore, we show that the relationship $\tau_y \approx \gamma_c G'$ is found in our experiments. The interaction between the vesicles and the vesicle deform-

ability are important for the macroscopic mechanical behavior. For the rheological behavior of dispersions of densely packed vesicles we have considered two limiting cases: dispersions of non-deformable interacting vesicles and dispersions of deformable vesicles which only interact at contact. For both cases estimates of the plateau value of G' were made. It is shown that both the repulsive vesicle interaction which results from thermal undulations and the vesicle deformation may be responsible for the observed G' values.

Further research on the rheological behavior of dispersions of vesicles that have bilayers consisting of unsaturated lipids may provide the answer to the question whether vesicle deformation or the inter vesicle interaction is responsible for the plateau value of the storage modulus. In principle both contribute to the storage modulus; however, the weakest of them contributes the most to the value of G' . This can be visualized as follows: In Figure 2 the influences of the deformability and the interaction on the elasticity of the entire dispersion are symbolized by different sets of springs. When two springs having a different modulus are connected to each other, the value of the effective modulus of the combined spring is close to that of the smallest modulus. Aging of unsaturated lipid bilayer vesicles results in a large decrease of the elastic membrane parameters^{2a} and the bending rigidity will decrease from about $25kT$ to order kT .^{10b} When vesicle deformation is responsible for G' it scales as $G' \propto k_c$ and when intervesicle interaction is responsible, it scales as $G' \propto k_c^{-1}$.

Acknowledgment. We thank Dr. M. Pâques of Unilever Research Laboratory Vlaardingen for preparing the freeze-fracture electron micrographs.

LA970564P